Plate Scale in Shaped Offset Gregorian Antennas

Dirk I. L. de Villiers and Robert Lehmensiek

Abstract – Shaped offset Gregorian antennas are used in several major radio telescope designs. The mapping function governing the relation between the feed pattern and reflector aperture distribution is typically designed for maximum receiving sensitivity under a set of additional beam pattern constraints. This article specifically investigates the effects of the mapping function on plate scale in these reflector systems. The plate scale value is not only a function of the subreflector subtended angle, as expected from classical conic section systems, but also a function of the aperture distribution resulting from the specific feed pattern and shaped mapping function. More uniform aperture distributions in flatter dishes produce smaller plate scale values. The implication is that the plate scale may become a conflicting requirement with maximum receiving sensitivity in electrically smaller dishes. In contrast, better sensitivity designs typically lead to smaller plate scale values for electrically large dishes.

1. Introduction

Radio astronomy reflector systems, like most of those used in point-to-point communication systems, are typically designed to maximize receiving sensitivity, while conforming to one or more other constraints on the primary (telescope) beam pattern [1]. These other constraints commonly involve a combination of, among others, maximum acceptable levels of cross polarization, sidelobe levels, beam circularity or symmetry, when the feed and reflectors are in nominal positions. To ensure that the systems remain operational in a range of environmental conditions, such as high winds and temperature variations due to differential heating, over the full antenna pointing domain with the associated gravitational deformations, it is important to design a system that is not too severely degraded by small shifts in the feed position. Such robust designs also allow simpler mechanical design and construction, as it places larger limits on acceptable feed position deviations from nominal cases.

For electrically very large reflectors (many hundreds of wavelengths in diameter), the effects of lateral and axial feed defocusing become more acute due to the simple problem of mechanically producing the multiscale reflector and support structure. In addition, modern telescopes, such as the MeerKAT [2], Square Kilometre Array [3], and Next-Generation Very Large Array (ngVLA) [4], all use offset Gregorian reflector systems to allow a feed indexer to be fitted at the focus, where multiple feed antennas can be moved into the focus to cover different frequency bands. The mechanical design of such a feed indexer results in physical limits on how accurately a feed can be positioned in the reflector focus. Several options exist to fine-tune the feed positions after indexing, and these are system specific and beyond the scope of this article. In general, though, errors in feed position degrade the primary beam of the system. In offset systems, both axial and lateral defocusing (in all axes) causes reduced aperture efficiency and a shift in the main beam direction [5–7].

In this article, we specifically investigate the effects of shaping the reflectors on a plate scale, which in optical telescope systems connects the angular separation of a distant object with the linear separation of its image on the focal plane. In radio reflectors (small diffraction-limited systems), the plate scale connects the feed position errors to the main beam pointing direction, where it is understood that in the nominal case, the main beam points at the reflector coordinate system zenith. This effect is also referred to as beam scanning [7], the beam deviation factor, or squint [5] in reflector antenna literature. Effects of the shaping mapping, which describes the aperture field distribution as a function of the feed radiation pattern, on aperture efficiency in scanned offset Gregorian systems are discussed in [7]. Similar studies were reported earlier in [6] for classical conic section systems. The work in this article differs from previous results in that we are not concerned with formally scanning the antenna beam here. Instead, we investigate the much smaller and more subtle effects of having feed antenna offsets present as a function of the shaping mapping. The scale of the antenna position errors is small enough to not cause a substantial loss in aperture efficiency, as is the case when scanning the beam several beamwidths. Instead, we show that the plate scale, or beam deviation factor, is a function of the reflector aperture field distribution (that is a function of the feed pattern and mapping function). In classical conic section reflectors (where the geometry fixes the mapping), flatter systems (smaller subtended angles) provide smaller plate scale values [5]. This is not generally true in shaped systems, for which one may have a smaller absolute plate scale in deeper systems if the mapping is correctly chosen. We will show how the plate scale trades with receiving sensitivity for a variety of offset Gregorian systems of different electrical sizes and with different subreflector ground shielding.

2. Reflector System Description

The reflector system under consideration is the 18 m class of shaped offset Gregorian systems under development for the ngVLA radio telescope. A suite of

Manuscript received 15 December 2021.

Dirk I. L. de Villiers and Robert Lehmensiek are with the Department of Electrical and Electronic Engineering, Bosman street, Stellenbosch, 7600, South Africa; e-mail: ddv@sun.ac.za.

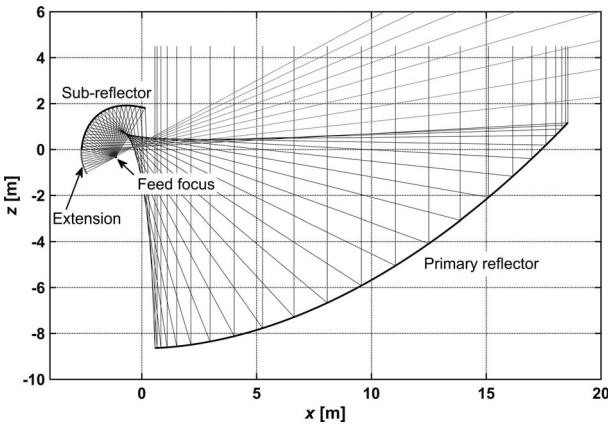

Figure 1. Offset Gregorian reflector geometry with dimensions representative of the 18 m ngVLA radio telescope. Also shown is the subreflector extension (with rays to cold sky) that reduces ground noise.

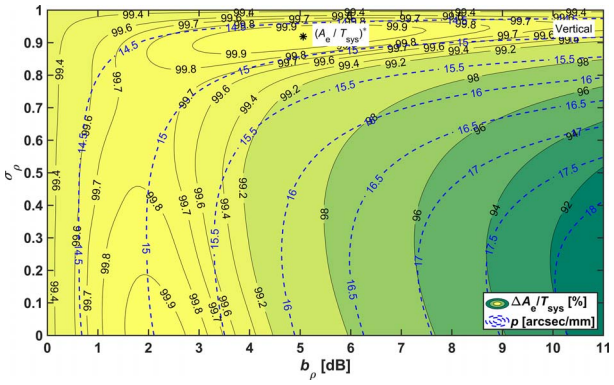

Figure 2. Contour plot of the normalized receiving sensitivity A_e/T_{sys} for the vertical polarization over the aperture field distribution parameter space at 30 GHz. The contour lines give the percentage value of the maximum value indicated by the asterisk. Superimposed (blue dashed contours) is the plate scale p.

cryogenic feeds mounted on an indexer mechanism at the reflector system's focus will have a frequency range extending from 1.2 GHz to 116 GHz. A symmetry plane cut of the reflector system is shown in Figure 1.

The shaping mapping function $\rho(\theta_f)$, with theoretical details described in [8], maps an axially given symmetric feed radiation power pattern $|G(\theta_f)|^2$ to an aperture field power distribution $|E(\rho)|^2$ through the relation

$$\rho(\theta_f)\rho'(\theta_f) = \frac{|G(\theta_f)|^2 \sin\theta_f}{V_c |E(\rho)|^2} \tag{1}$$

where $\rho'(\theta_f)$ denotes the θ_f derivative of ρ and V_c is a normalization constant. This mapping function maps constant cones of the feed angle θ_f to circles of constant radius ρ in the aperture. Here, the mapping function is determined from an actual feed pattern (averaged over ϕ_f) and a parameterized aperture field distribution. The feed is an axially symmetric corrugated wide-flare-angle conical horn designed for pattern symmetry and high spillover efficiency. The horn's bandwidth is approximately 1.66:1 and has an edge taper close to −16 dB. The aperture field distribution is modeled as a hybrid uniform Gaussian function, i.e.,

$$|G(\theta_f)|^2 = \begin{cases} 1, & 0 \le \rho \le \sigma_\rho \rho_m \\ \exp\left[-b_\rho \left(\frac{\rho - \sigma_\rho \rho_m}{\rho_m (1-\sigma_\rho)}\right)^2\right], & \sigma_\rho \rho_m \le \rho \le \rho_m \end{cases} \tag{2}$$

The constant b_ρ controls the edge taper, and σ_ρ controls the extent of the central uniform power distribution. A two-dimensional space spanning a range of b_ρ and σ_ρ is, thus, investigated as mapping functions for the reflector system.

The subreflector is extended to reduce the ground noise contribution to the antenna temperature, as shown in Figure 1. This extension dramatically improves the noise performance of offset Gregorian systems tipping in the feed down configuration, where the subreflector moves closer to the ground, as the beam scans toward the horizon [9].

3. Simulation Results

A range of parametric sweeps was performed to estimate the performance of the system for different subreflector subtended angles, mapping functions, and subreflector extensions. In all cases, the actual feed pattern (with spherical wave expansion to model near-field effects) was used to illuminate the reflector system in the physical optics analysis package GRASP, version 20.0 [10]. The receiving sensitivity A_e/T_{sys} (ratio of effective aperture area to system temperature) was calculated by using the reflector masking techniques described in [11, 12]. The receiver noise temperature is varied according to the frequency band of interest (the receivers will be cryogenically cooled, with a value of 16 K at 30 GHz). An atmospheric model representative of typical conditions at the proposed site of the telescope in New Mexico is used in the brightness temperature model, adapted from the model given in [13].

Figure 2 shows the receiving sensitivity over the entire mapping function parameter space. Results are only shown for a 55° subtended angle subreflector, because they are similar for the 45° and 50° cases investigated here. The left ($b_\rho = 0$) and top ($\sigma_\rho = 1$) part of the graph is the uniform aperture field distribution, while the bottom part ($\sigma_\rho = 0$) on the graph is the purely Gaussian distribution. High receiving sensitivity is found on a contour just off uniform aperture field distribution, i.e., with a little bit of reduced energy at the edge of the aperture to reduce spillover. The plate scale contours p, indicated in arcsecond of beam squint per millimeter of lateral feed displacement in the symmetry plane of the system, are superimposed on the sensitivity contour plot and follow similar trends as the sensitivity contours. The lowest plate scale is observed for a uniform aperture field distribution, and it progressively

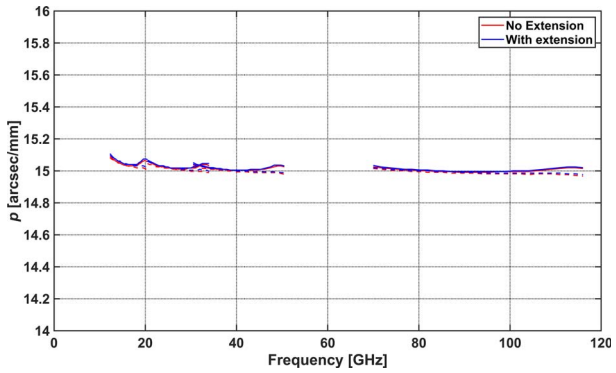

Figure 3. Plate scale as a function of frequency for a subreflector with and without an extension. The mapping function has $b_\rho = 2.1$ and $\sigma_\rho = 0$. Both the vertical (solid) and horizontal (dashed) polarizations are shown.

becomes worse as the aperture field distribution becomes more Gaussian with a higher edge taper.

The plate scale is relatively constant over frequency (and thus electrical size of the system), as shown in Figure 3. Here, the corrugated horn is scaled to the four frequency bands shown in the figure. The slight variation observed over frequency is due to the actual feed's pattern variation over frequency, which, in turn, causes slight variations in the aperture field distribution. At lower frequencies, diffraction will also have an impact on the plate scale. Results are shown for subreflectors with and without an extension. Because the extension has little effect on the aperture field distribution, it has virtually no impact on the plate scale.

From the plots previously mentioned, it is clear that the plate scale is a strong function of the feed pattern and mapping function, i.e., the aperture field distribution. A more uniform aperture field distribution is better for plate scale, which is why flatter dishes in classical conic section systems have better plate scale. For shaped systems, the subreflector subtended angle, therefore, does not play a significant role in the plate scale of the system.

4. References

1. R. Lehmensiek, I. P. Theron, and D. I. L. de Villiers, "Deriving an Optimum Mapping Function for the SKA-Shaped Offset Gregorian Reflectors," *IEEE Transactions on Antennas and Propagation*, **63**, 11, November 2015, pp. 4658-4666.
2. J. L. Jonas, "MeerKAT—The South African Array with Composite Dishes and Wide-Band Single Pixel Feeds," *Proceedings of the IEEE*, **97**, 8, August 2009, pp. 1522-1530.
3. P. E. Dewdney, P. J. Hall, R. T. Schilizzi, and T. J. L. W. Lazio, "The Square Kilometer Array," *Proceedings of the IEEE*, **97**, 8, August 2009, pp. 1482-1496.
4. R. Selina, "The Next-Generation Very Large Array: Reference Design Overview," URSI Asia-Pacific Radio Science Conference, New Delhi, India, March 9–15, 2019, pp. 1-1.
5. J. Ruze, "Lateral-Feed Displacement in a Paraboloid," *IEEE Transactions on Antennas and Propagation*, **13**, 5, September 1965, pp. 660-665.
6. O. Sørensen and W. V. T. Rusch, "Application of the Geometrical Theory of Diffraction to Cassegrian Subreflectors with Laterally Defocused Feeds," *IEEE Transactions on Antennas and Propagation*, **23**, 5, September 1975, pp. 698-702.
7. V. Galindo-Israel, W. Veruttipong, R. D. Norrod, and W. A. Imbriale, "Scanning Properties of Large Dual-Shaped Offset and Symmetric Reflector Antennas," *IEEE Transactions on Antennas and Propagation*, **40**, 4, April 1992, pp. 422-432.
8. P.-S. Kildal, "Synthesis of Multireflector Antennas by Kinematic and Dynamic Ray Tracing," *IEEE Transactions on Antennas and Propagation*, **38**, 10, October 1990, 1587-1599.
9. D. I. L. de Villiers and R. Lehmensiek, "Sub-Reflector Extensions for Reduced Noise Temperature in Low-Side Sub-Reflector Offset Gregorian Systems," Sixth European Conference on Antennas and Propagation, Prague, Czech Republic, March 2012, pp. 3438-3441.
10. TICRA, *GRASP20*, version 20.0, Copenhagen, Denmark, TICRA, http://www.ticra.com, 2022.
11. D. I. L. de Villiers and R. Lehmensiek, "Rapid Calculation of Antenna Noise Temperature in Offset Gregorian Reflector Systems," *IEEE Transactions on Antennas and Propagation*, **63**, 4, April 2015, pp. 1564-1571.
12. R. Lehmensiek and D. I. L. de Villiers, "Noise Temperature Approximations for Offset Gregorian Reflector Systems," *IEICE Transactions on Communications*, **E101-B**, 2, February 2018, pp. 332-339.
13. G. C. Medellín, *Antenna Noise Temperature Calculation*, memo no. 95, US SKA Technology Development Project, Ithaca, NY, July 2007.